NATIONAL ADVISORY COMMITTEE FOR AERONAUTICS

TECHNICAL NOTE 4354

MEASUREMENTS IN A SHOCK TUBE OF HEAT-TRANSFER RATES AT THE STAGNATION POINT OF A 1.0-INCH-DIAMETER SPHERE FOR REAL-GAS TEMPERATURES UP TO 7,900° R

By Alexander P. Sabol

Langley Aeronautical Laboratory
Langley Field, Va.

Washington
August 1958

NATIONAL ADVISORY COMMITTEE FOR AERONAUTICS

TECHNICAL NOTE 4354

MEASUREMENTS IN A SHOCK TUBE OF HEAT-TRANSFER RATES AT THE STAGNATION POINT OF A 1.0-INCH-DIAMETER SPHERE FOR REAL-GAS TEMPERATURES UP TO 7,900° R

By Alexander P. Sabol

SUMMARY

Heat-transfer rates at the stagnation point of 1.0-inch-diameter glass spherical models have been measured in shock-tube flows in air which corresponded to free-flight conditions between Mach numbers of 6.4 and 13.9 with stagnation temperatures up to 7,900° R. The heat-transfer rates were determined from measurements of the surface-temperature change with time of a thin-film-platinum resistance thermometer. The test results are presented and compared with the results from the theories of Lees (Jet Propulsion, April 1956) and Fay and Riddell (AVCO Research Report 1). The experimental results obtained give lower heat-transfer rates than both theories but are more compatible with results from the theory of Lees. These test results are also compared with thermocouple data and with the results obtained by the use of similar configurations.

INTRODUCTION

Many aerodynamic problems of hypersonic flight, such as the heat-transfer rate at the stagnation point, can be studied in a shock tube. This problem is of interest at present and is amenable to investigation because the shock tube can generate the high temperatures necessary to simulate hypersonic conditions. For investigations of the heat-transfer rate at the stagnation point, only the stagnation enthalpy and pressure need be duplicated. The difference between the flight and test Mach numbers can be neglected if the external flow fields are similar. These conditions can be obtained in the straight portion of the tube for a limited flow region behind the primary shock wave. A series of tests were therefore made in a high-pressure shock-tube facility in the Langley Gas Dynamics Branch to obtain heat-transfer rates at the stagnation point for a range of conditions available in a shock tube. These tests were made with a fast responding, thin-film-platinum resistance thermometer mounted on the surface of a 1-inch-diameter glass model. The results of several tests are presented and show the heat-transfer rates

at the stagnation point obtained for conditions corresponding to a range in free-flight Mach number from 6.4 to 13.9 at high altitudes. The experimental results are compared with the theoretical results based on the work of Lees (ref. 1) and Fay and Riddell (ref. 2). These results are discussed to show compatibility with the experimental results of Rose and Stark (ref. 3) and with the results of similar tests made with the use of a surface thermocouple element of the same order of thickness as the thin-film thermometer. The thermocouple data were obtained in a previous investigation by Morton Cooper and Jim J. Jones of the Langley Aeronautical Laboratory.

SYMBOLS

c	specific heat of glass, 0.20 Btu/lb-$^{\circ}$F
e	current intensity, volts
h	enthalpy of air, Btu/lb
i	current, amp
k	diffusivity of glass, 6.67×10^{-6} sq ft/sec
M	Mach number
p	pressure, atm
Q	heat-transfer rate, Btu/sq ft/sec
R	resistance, ohms
N_{Re}	Reynolds number, based on model diameter
t	time, sec
T	temperature, $^{\circ}$R
$T(t)$	surface-temperature rise as a function of time, $^{\circ}$R
ρ	unit weight of glass, 139.2 lb/cu ft

Subscripts:

0	stagnation region behind shock; also refers to sensitive element
1	region ahead of primary shock

2	region behind primary shock
3	region behind stationary model bow shock
a	assumed value
e	experiment
s	related to primary shock
th	related to theory
w	wall condition

APPARATUS AND EXPERIMENTAL METHODS

Heat-transfer measurements were made in a $3\frac{3}{4}$- inch-diameter shock tube with air as the test medium. A shock in the tube was generated by bursting metal diaphragms with high-pressure helium or hydrogen gas. When the resulting shock wave reached the model the temperature measurements began and continued for the duration of the approximately steady flow which followed. A more complete description of the shock tube, of the instrumentation, and of the flow details behind the primary shock wave is given in reference 4. The test models were located 68.15 feet from the diaphragm station and, in order to prevent shock reflections, the shock tube extended an additional 60 feet from the model.

The wave velocity of the primary shock was measured at 10 locations in the tube by use of both ionization and pressure sensitive probes. For conditions where weak shock waves failed to trip ionization probes, several ionization probes were replaced by pressure transducers. Signals from all these instruments were detected by electronic interval counters or on an oscillograph to record time of shock passage. Shock strengths were varied by changing the driver gas, the driver-gas pressure, and the air pressure in the low-pressure section of the tube. Air pressures in the low-pressure section from approximately 0.45×10^{-2} to 9.9×10^{-2} atmosphere were used.

Figure 1 is a photograph of typical models used. The models were formed into hollow 1.0-inch-diameter partial spheres at the end of a 3/4-inch-outside-diameter and 1/2-inch-inside-diameter pyrex glass tubing. In the vicinity of the stagnation point and extending rearward 45° from the stagnation point, the radius of the sphere had a tolerance of ± 0.01 inch.

The surface-temperature rise with time at the model stagnation point was determined by measuring the resistance change of a sensitive element, or the thin-film thermometer. The sensitive element measured 1/8 by 1/8 inch and consisted of a single thin coating of Hanovia Liquid Bright Platinum No. 05 which was applied to the model in the same manner as that described in reference 5. The resulting sintered film had an approximate thickness of about 4×10^{-6} inch and an electrical resistance of about 16 ohms per square inch. This thermometer was resistant to abrasion by the flow and had a rapid response to temperature changes (ref. 6). Means were provided for conducting electrical signals from the sensitive element to instrumentation outside the shock tube through several leads that passed into the supporting tube of the model. (See fig. 1.) In order to minimize surface roughness behind the stagnation point, thin silver leads were applied to the surface to join the sensitive element with wire leads that entered the supporting tube. The silver leads were made from a liquid silver paste and were applied with the same technique as that used for the platinum paste. The leads had a low resistance relative to the sensitive element. They were subsequently covered with one coating of clear insulating paint to help prevent detecting stray electrical signals. These insulated leads had an average measured thickness of 0.0015 inch. The wire leads in the supporting tubing connected to the silver leads 90° behind the stagnation point, and four silver leads joined to the element. Two of these leads were current-carrying, while the other two were voltage-measuring leads - a technique used earlier in the investigation of reference 3. Figure 2 is a schematic drawing of the electrical circuit which connected to the sensitive element. In the circuit a 200-ohm resistor center tapped to ground was joined parallel to the thermometer to provide a balanced drain-off for any stray signal.

The sensitive element was calibrated before each test by immersing the model in heated silicone oil and noting the resistance of the element for various temperatures of the oil. During a test, the resistance change of the sensitive element on the model was measured by noting the voltage drop across the element for a current of approximately 10.0 milliamperes through it. This current was found to produce undetectable heating of the element when the model was placed in the testing environment. The changing voltage at the sensitive element was amplified, fed into the vertical axis of a cathode-ray oscillograph, and recorded by a film-drum camera. A camera film speed of 1.0 inch per millisecond was maintained by a synchronous motor. A typical voltage-time record produced by the sensitive element is shown in figure 3 from which both the voltage rise $\Delta e(t)$ and time elapsed t were obtained.

As a result of bombardment of the model by fine particles in the flow, each model was used for only one test, although on occasions where the damage to the model was slight, as for the case of low-velocity flows,

the models were recalibrated for a second test. Fine particles were unavoidably present in the flow but it is believed that they reached the model only after the termination of steady flow.

The thermocouple models of the previous tests of Morton Cooper and Jim J. Jones were solid glass spheres. The thermocouple was formed by evaporating onto the glass a compound band of overlapping nickel and silver which joined at the nose of the model. The electrical circuit joining the thermocouple with a voltage preamplifier and recorder consisted only of a series resistor which compensated for differences in resistance between the leads from the preamplifier to the ends of the thermocouple proper. The thickness of the thermocouple was roughly determined to be 4×10^{-6} inch. The method of calibrating the thermocouple paralleled that of the thin-film thermometer. Unlike the thin-film thermometer, however, the thermocouple could be used for repeated tests without recalibration. The thermocouple readings were unaffected by abrasion and pitting during a test. All the tests with the thermocouple model were made with an air pressure of 0.566×10^{-2} atmosphere in the low-pressure chamber of the shock tube.

DATA REDUCTION

The surface-temperature rise at the stagnation point on the models was determined from the resistance change of the thin-film thermometer. If the relatively small resistance of the short wire leads to the instrumentation is neglected the current through the sensitive element, before a test, is approximately

$$i_0 = i - \frac{e}{200}$$

where e represents the voltage observed at the sensitive element and i, the battery current measured by use of a standard resistor (fig. 2). The calibration of the sensitive element showed a linear resistance change with temperature and the test conditions did not exceed the upper calibrated temperature; therefore, the test-temperature change with time of the element could be obtained from the following equation:

$$T(t) = \frac{\Delta e(t)}{i_0} \left(\frac{\Delta T}{\Delta R_0}\right)_{\text{calibrated}}$$

During a test the current i_0 changed a negligible amount due to the resistance change of the sensitive element.

In order to determine the heat-transfer rate at the stagnation point, a sensitive element of negligible thickness was used, that is,

approximately 4×10^{-6} inch (approximately 1.0 micron). This thickness permitted the element to register nearly the true surface-temperature rise of the model (ref. 6). It also permitted, in computing the heat-transfer rate, approximation of the stagnation region as a semi-infinite solid when the running time was relatively short. With a large temperature difference between the air and the model and with a region of approximately steady flow behind the primary shock wave, the heat-transfer rate to the model for the first few instances of time could be considered constant. The heat-transfer rate could then be obtained from

$$Q_e = \frac{T(t)}{2\sqrt{t}} \sqrt{\pi k \rho c} \tag{1}$$

As seen from equation (1) the behavior of the function $T(t)$ varies as the square root of time t. An actual voltage record is shown in figure 3.

Shock-tube flows generated by the primary shock are not ideally steady. Slight flow variations are sometimes present which affect the heat-transfer rate. Under these conditions, the heat-transfer rate can be described by

$$Q(t) = \frac{\sqrt{\pi k \rho c}}{\pi} \left[\frac{T(t)}{\sqrt{t}} + \frac{1}{2} \int_0^t \frac{T(t) - T(\tau)}{(t - \tau)^{3/2}} \, d\tau \right] \tag{2}$$

which was derived from one-dimensional unsteady heat flow conditions. Although a constant heat-transfer rate was anticipated, the calculations were made by using equation (2) as a verification. Numerical calculation of this integral is complicated by the behavior of the integrand for values of the dummy variable τ close to t. By terminating the integration at some value of $\tau = t_a < t$, reasonable accuracy could be maintained when the rest of the integral was approximated by assuming that T was a linear function over the interval t_a to t. This approximation leads to:

$$Q(t) = \frac{\sqrt{\pi k \rho c}}{\pi} \left[\frac{T(t)}{\sqrt{t}} + \frac{1}{2} \int_0^{t_a} \frac{T(t) - T(\tau)}{(t - \tau)^{3/2}} \, d\tau + \frac{dT(t)}{dt} (t - t_a)^{1/2} \right] \tag{3}$$

By comparing the altered integration method (eq. (3)) with the exact method for the case of constant $Q(t)$ (eq. (2)), a value of $t_a = 0.9t$ was found to maintain the accuracy of the numerical integration but changed the value of $Q(t)$ by only 4 percent, a constant which could be accounted for in the result. Simpson's approximation rule was then used to compute the integral in equation (3), and in the last term,

$\frac{dT(t)}{dt}$ was the average slope between t_a and t. Bulk properties of the particular glass were used for k, ρ, and c. The heat-transfer results obtained are presented in table I(a) with the calculated real-gas flow conditions and in figure 4 which shows the variation of heat-transfer rate with time. For comparison, table I(b) shows the flow conditions of air calculated for a constant ratio of specific heat of 1.4. As can be seen there is significant difference between the real and ideal stagnation-point conditions.

Calculations of the flow conditions were based on the measured pressure, temperature of the air ahead of the primary shock, and the shock velocity. Rankine-Hugoniot conservation relations were then used in an iteration process to determine all the flow conditions. Real-gas properties for equilibrium conditions were used from reference 7 to obtain table I(a). The value of the dissociation energy of nitrogen used was incorrect but introduced only a small error in the calculated properties of air up to 7,900° R, since at the stagnation pressures the amount of nitrogen dissociation was small.

The experimental values of the heat-transfer rate are compared in figure 5 with theoretical results from the theories of Lees (ref. 1) and Fay and Riddell (ref. 2). In the application of both theories a velocity gradient based on the Newtonian values $\left(\frac{2p_0}{\rho_0}\right)^{1/4}$ was used, and real-gas properties were also considered in the theories. A Lewis number of 1.4 was used in the theory of Fay and Riddell, and the theory of Lees was multiplied by $\frac{h_e - h_w}{h_0}$.

RESULTS AND DISCUSSION

After the primary shock wave passed the model, a region of comparatively steady flow was established in which tests were made. The duration of this steady flow could be determined from the regularity of the voltage rise at the sensitive element. (See fig. 3.) This duration was longest for the low shock strengths, of the order of 0.5 millisecond, and shortest for the high shock strengths, approximately 0.1 millisecond. Reference 4 shows the running times available at other stations in the shock tube. Figure 4 shows the heat-transfer rates obtained at different time intervals. An apparent sharp rise in the heat-transfer rate, which is illustrated as a typical case, was attributed to a particle hitting the model. The heat-transfer rates varied from 240 to 1,297 Btu/sq ft/sec for real-

gas stagnation temperatures that varied from 3,300° to 7,900° R. Since a longer test time tends to give more accuracy in the determined heat-transfer rate (see ref. 6) the heat rates at $t = 0.22$ millisecond were selected for comparison with theory for all but the case of highest heat rate; these rates are tabulated in table I(a). Also included in this table are the results of calculations made by approximating the measured heat input as a constant rate.

Figure 5 shows the comparison of the experimental heat-transfer rates obtained with those from application of the theories of Lees and Fay and Riddell by indicating the respective ratios. These ratios are plotted against free-flight Mach numbers which are the flight speeds required in a standard atmosphere (ref. 8) to duplicate the stagnation pressures and temperatures of the shock-tube tests. The test conditions corresponded to the Mach number range from $M = 6.4$ to 13.9 and to the altitude range between 40,000 and 95,000 feet. The maximum heat-transfer rate of 1,297 Btu/sq ft/sec occurred with a stagnation condition that corresponded to a free-flight Mach number of 13.9.

Figure 5 shows that the results obtained with the thin-film thermometer average from 0 to 30 percent less than the results calculated by use of the theory of Lees and from 20 to 40 percent less than the results calculated by use of the more accurate theory of Fay and Riddell. The thermocouple results of Cooper and Jones indicate better agreement with the theory of Fay and Riddell, the average of those results being 10 percent less than the theoretical results. The results of reference 3 agree favorably with the results from the theory of Fay and Riddell. There appears to be no apparent reason for the relatively lower values of the present test results. Precaution was taken to measure the heat-transfer rates at surface temperatures within the calibration range of the thin-film thermometer. As a note of interest, if the value of the Lewis number in the theory of Fay and Riddell were changed from 1.4 to 1.0, this would lower the theory curve in figure 5 by not more than 5 percent.

CONCLUDING REMARKS

Heat-transfer rates at the nose of 1.0-inch-diameter models were measured in a shock tube with flow stagnation temperatures up to 7,900° R by using a thin-film-platinum resistance thermometer. The maximum heat-transfer rate obtained was 1,297 Btu/sq ft/sec which corresponded to a free-flight Mach number of 13.9.

The results of the present tests average approximately 20 to 40 percent lower than the results from the theory of Fay and Riddell (AVCO Research Report 1) but are more compatible with the results from the

theory of Lees (Jet Propulsion, April 1956), being from 0 to 30 percent lower. These test results also show lower heat-transfer rates than those obtained by use of a thermocouple and those obtained by Rose and Stark (AVCO Research Report 3).

Langley Aeronautical Laboratory,
National Advisory Committee for Aeronautics,
Langley Field, Va., June 18, 1958.

REFERENCES

1. Lees, Lester: Laminar Heat Transfer Over Blunt-Nosed Bodies at Hypersonic Flight Speeds. Jet Propulsion, vol. 26, no. 4, Apr. 1956, pp. 259-269.

2. Fay, J. A., and Riddell, F. R.: Theory of Stagnation Point Heat Transfer in Dissociated Air. Res. Rep. 1, AVCO Res. Lab., June 1956 (rev. Apr. 1957). (Formerly AVCO Res. Note 18.)

3. Rose, P. H., and Stark, W. I.: Stagnation Point Heat Transfer Measurements in Dissociated Air. Res. Rep. 3, AVCO Res. Lab., Apr. 1957. (Formerly AVCO Res. Note 24.)

4. Jones, Jim J.: Experimental Investigation of Attenuation of Strong Shock Waves in a Shock Tube With Hydrogen and Helium as Driver Gases. NACA TN 4072, 1957.

5. Vidal, R. J.: Model Instrumentation Techniques for Heat Transfer and Force Measurements in a Hypersonic Shock Tunnel. Rep. No. AD-917-A-1 (Contract No. AF 33(616)-2387), Cornell Aero. Lab., Inc., Feb. 1956. (Available from ASTIA as AD-97238.)

6. Vidal, Robert J.: A Resistance Thermometer for Transient Surface Temperature Measurements. Presented at the Am. Rocket Soc. Meeting (Buffalo), Sept. 24-26, 1956.

7. Anon.: Handbook of Supersonic Aerodynamics. NAVORD Rep. 1488 (vol. 5), Bur. Ord., Aug. 1953.

8. The Rocket Panel: Pressures, Densities, and Temperatures in the Upper Atmosphere. Phys. Rev., vol. 88, no. 5, Second ser., Dec. 1, 1952, pp. 1027-1032.

TABLE I.- TEST CONDITIONS

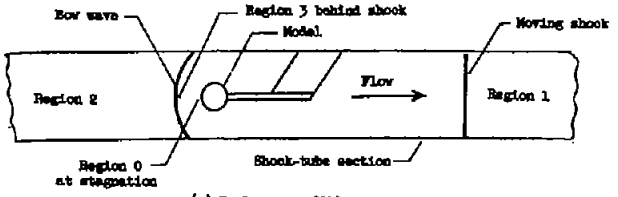

(a) Real-gas conditions

Test points from figure 4	p_1, atm	T_1, °R	M_s	p_2, atm	T_2, °R	M_2	$R_{e,2}$	p_3, atm	T_3, °R	M_3	p_0, atm	T_0, °R	q_a, Btu/sq ft/sec	q_a, Btu/sq ft/sec (a)
○	9.92×10^{-2}	538	4.22	2.08	2,257	1.71	3.61×10^5	6.70	3,060	0.628	8.48	3,256	240	226
□	8.68	510	4.41	1.99	2,270	1.73	3.45	6.56	3,133	.622	8.25	3,307	307	313
◇	3.89	539	5.46	1.39	3,268	1.92	1.72	5.62	4,070	.576	6.90	4,833	543	450
△	1.84	540	5.93	.777	3,716	1.99	.852	5.40	5,220	.557	4.00	5,355	487	526
▽	2.28	532	6.38	1.12	4,087	2.05	1.12	5.22	5,680	.536	6.20	5,796	491	514
◭	.947	536	6.40	.469	4,120	2.07	.468	2.26	5,638	.530	2.63	5,742	477	468
◻	1.99	532	6.69	1.08	4,362	2.11	1.02	5.89	5,980	.520	6.27	6,109	585	581
◇	2.04	532	7.04	1.30	4,842	2.20	1.13	6.90	6,512	.499	7.80	6,622	765	684
○	1.01	530	7.35	.655	4,868	2.25	.579	3.62	6,445	.487	4.37	6,570	643	625
◇	1.99	504	7.84	1.50	5,135	2.29	1.26	8.50	6,880	.489	9.70	6,998	969	862
◇	.447	525	8.32	.365	5,364	2.46	.322	2.48	7,040	.451	2.78	7,146	692	662
△	.618	522	9.14	.646	5,850	2.58	.508	4.58	7,843	.440	5.02	7,934	1,297	1,336

[a]Based on a constant rate of heat input.

(b) Ideal-gas conditions, $\gamma = 1.4$

Test points from figure 4	p_1, atm	T_1, °R	M_s	p_2, atm	T_2, °R	M_2	$R_{e,2}$	p_3, atm	T_3, °R	M_3	p_0, atm	T_0, °R
○	9.92×10^{-2}	538	4.22	2.05	2,368	1.58	3.18×10^5	5.64	3,260	0.674	7.65	3,553
□	8.68	510	4.41	1.95	2,404	1.61	3.02	5.54	3,345	.667	7.46	3,642
◇	3.89	539	5.46	1.35	3,627	1.69	1.36	4.28	5,274	.642	5.65	5,708
△	1.84	540	5.93	.732	4,198	1.72	.651	2.44	6,156	.655	3.25	5,685
▽	2.28	538	6.38	1.08	4,711	1.74	.889	3.64	7,017	.650	4.75	7,374
◭	.947	536	6.40	.452	4,781	1.74	.342	1.55	7,128	.650	2.00	7,689
◻	1.99	532	6.69	1.05	5,130	1.76	.727	3.54	7,685	.627	4.63	8,288
◇	2.04	532	7.04	1.24	5,917	1.77	.751	4.35	8,951	.622	5.65	9,642
○	1.01	530	7.35	.632	6,003	1.78	.375	2.22	9,189	.622	2.89	9,892
◇	1.99	504	7.84	1.43	6,702	1.79	.782	5.10	9,915	.619	6.61	10,675
◇	.447	525	8.32	.561	7,556	1.80	.168	1.51	11,543	.616	1.69	12,423
△	.618	522	9.14	.601	8,959	1.88	.251	2.21	15,824	.615	2.85	14,870

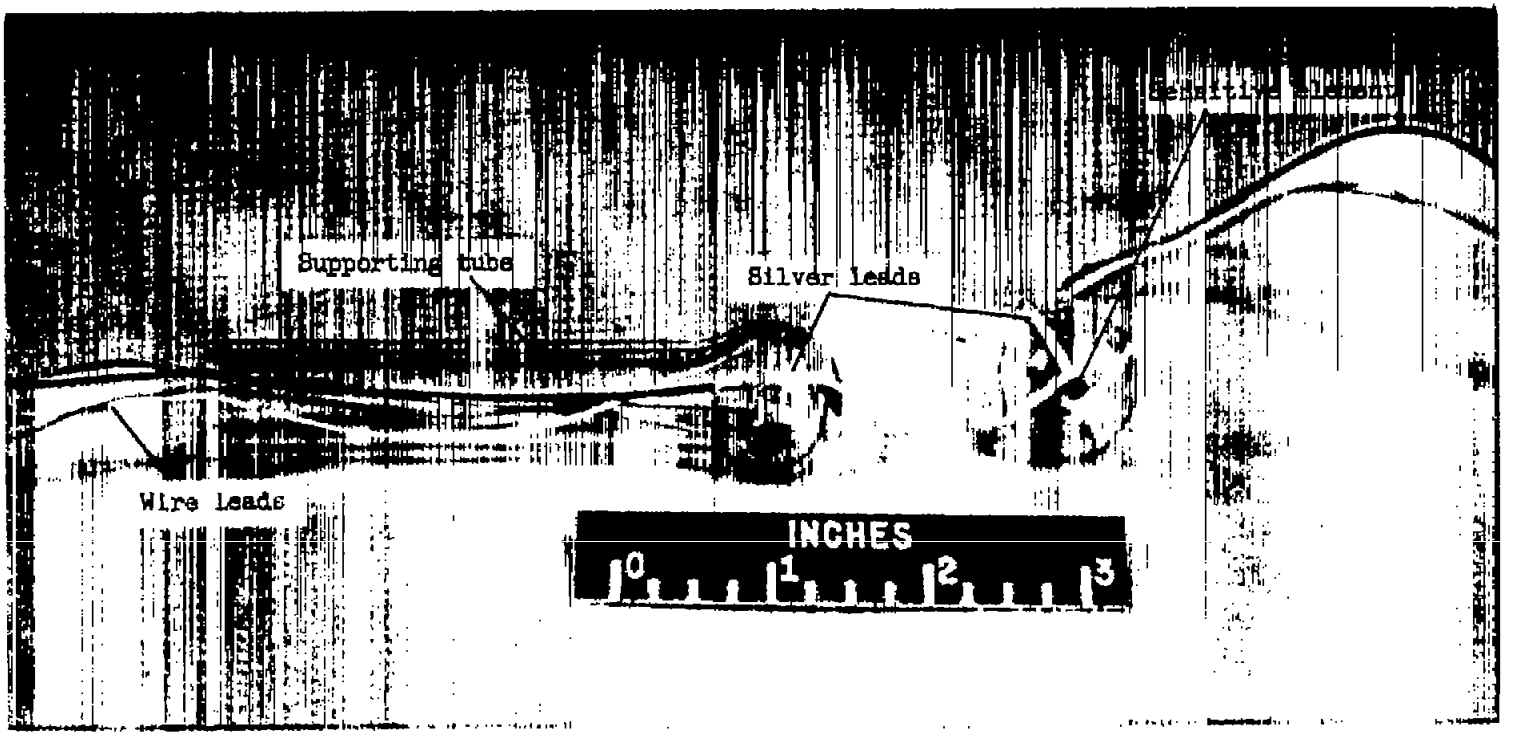

Figure 1.- Shock-tube heat-transfer models. L-57-235.1

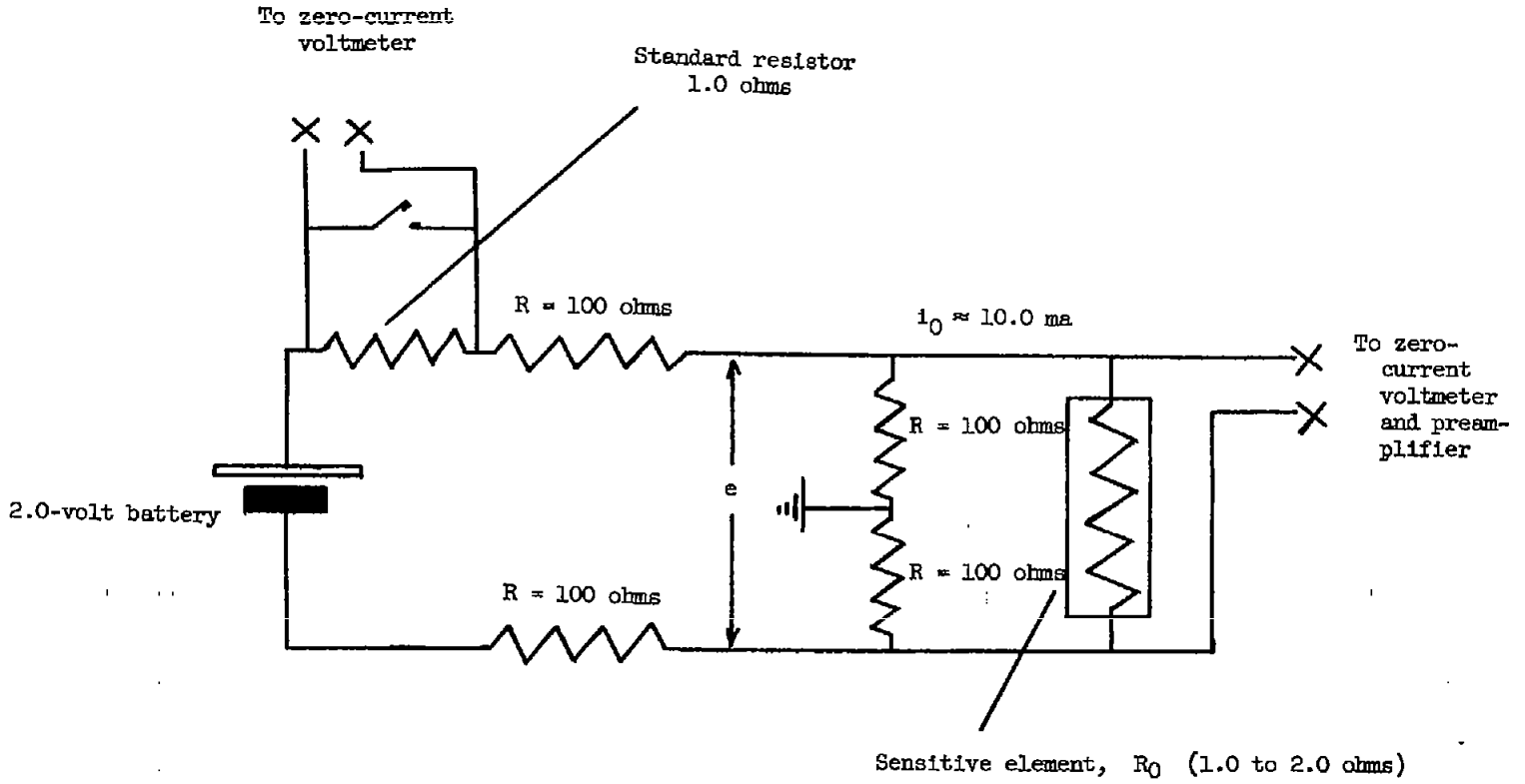

Figure 2.- Schematic diagram of electrical circuit used in measuring resistance change of stagnation-point thermometer.

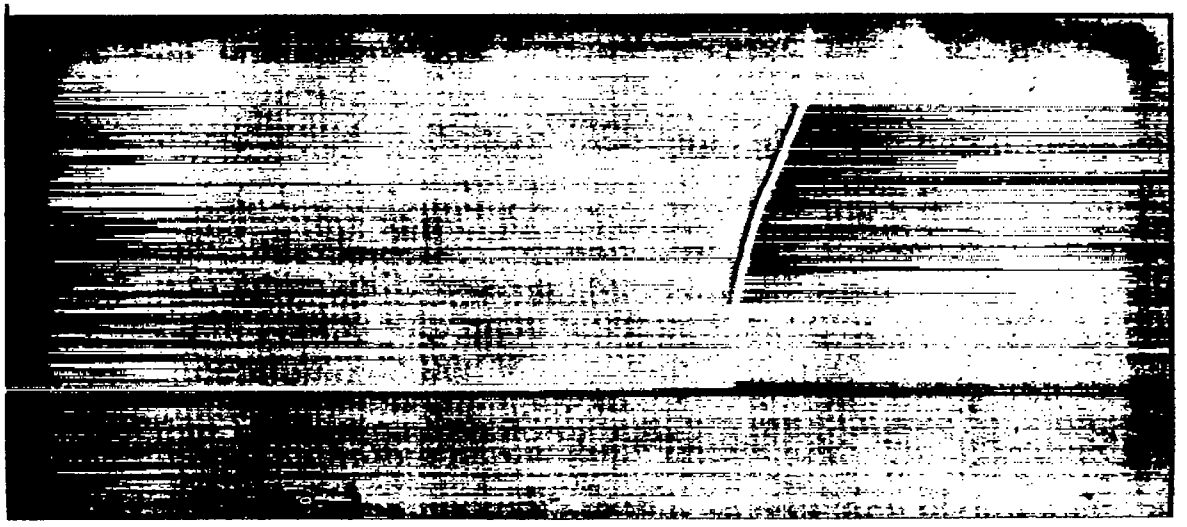

Figure 3.- A typical record showing voltage rise with time at the sensitive element. Film speed, 1.0 inch per millisecond.

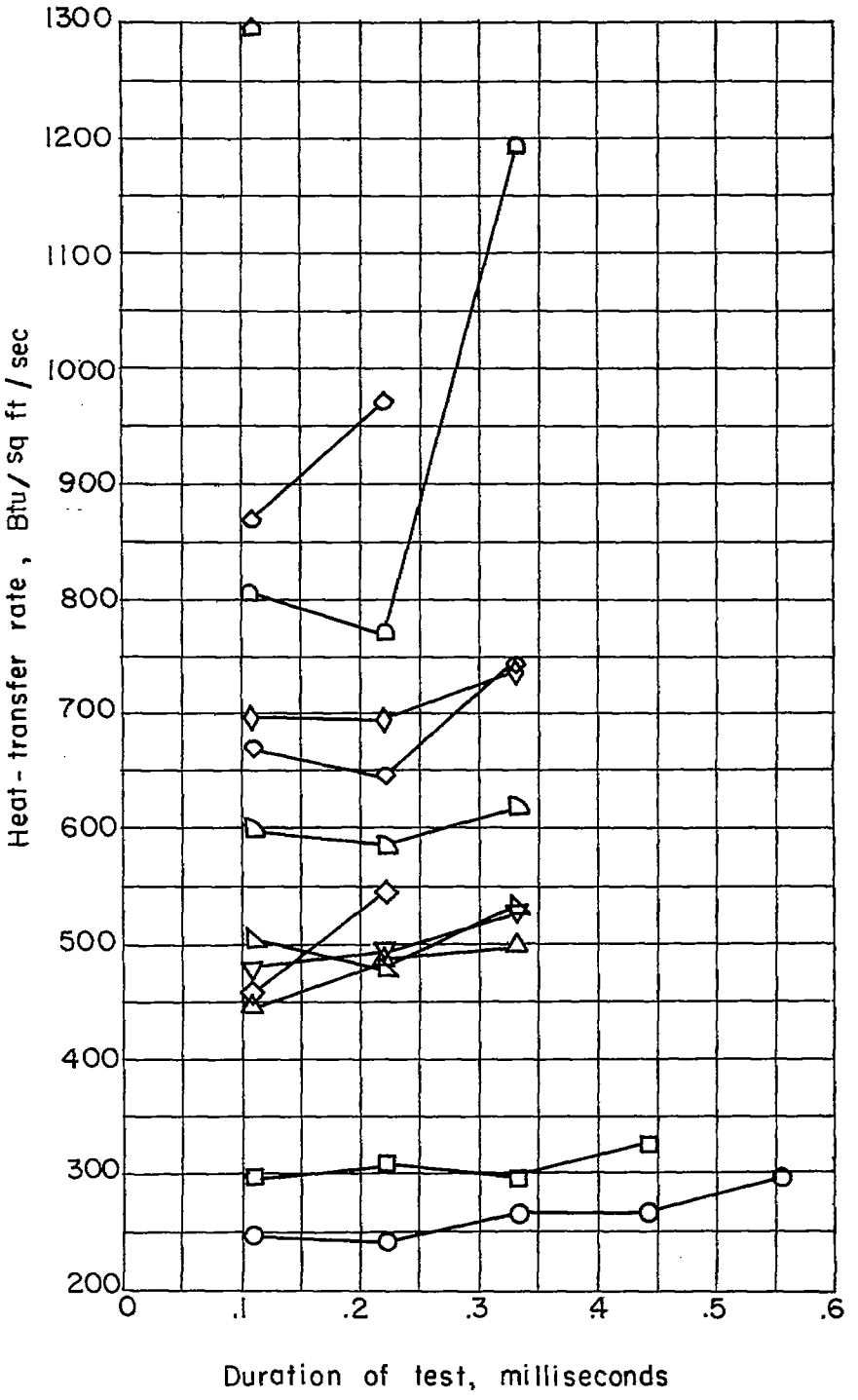

Figure 4.- Observed heat-transfer rates for 0.5-inch nose radius.

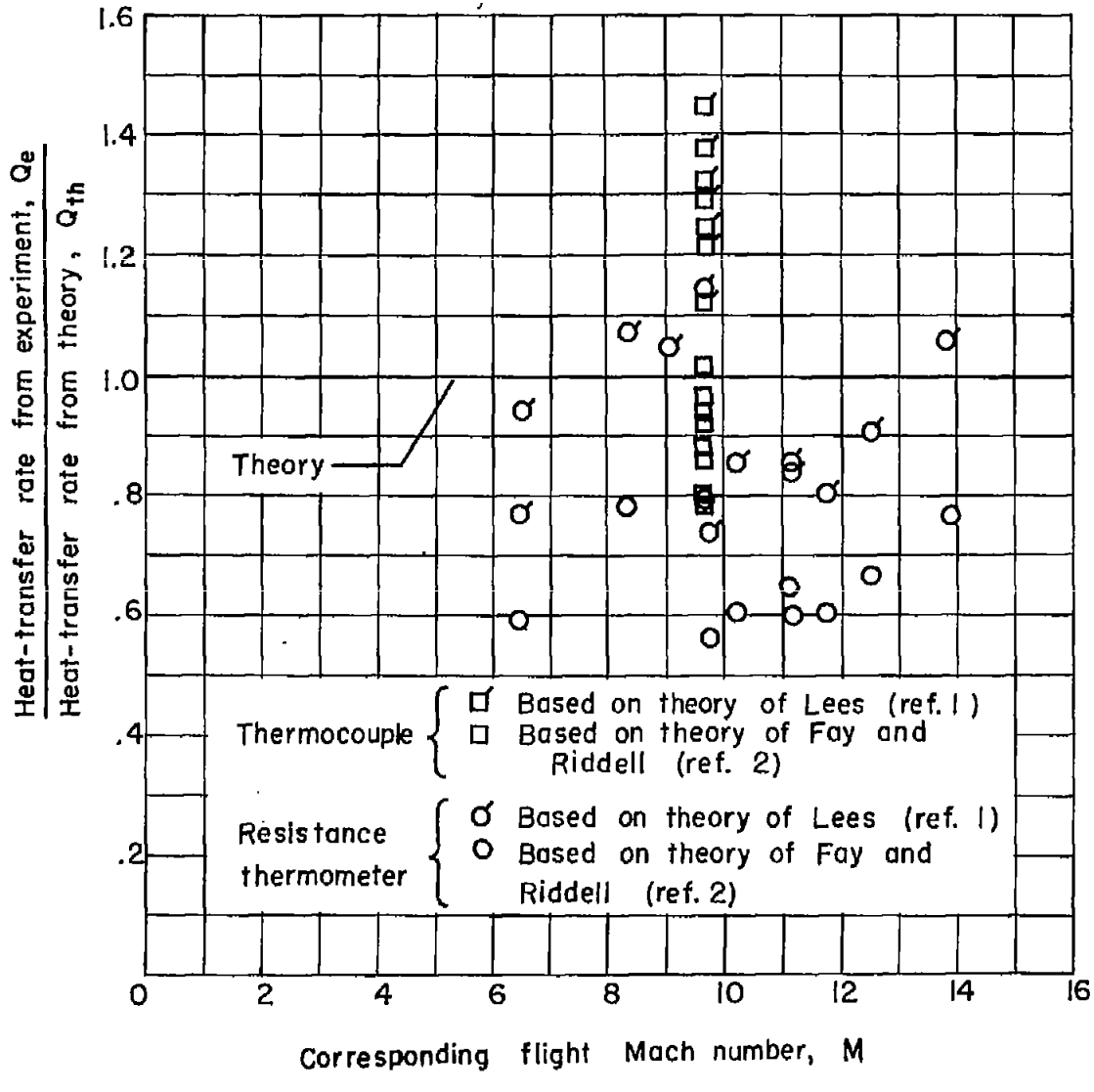

Figure 5.- Heat-transfer rate at stagnation point compared with rates calculated from theory.